Pharmacokinetic Modeling and Simulation with Pharmacogenetic Insights Support the Relevance of Therapeutic Drug Monitoring for Myeloablative Busulfan Dosing in Adult HSCT

Khalil Ben Hassine, Claire Seydoux, Sonia Khier, Youssef Daali, Michael Medinger, Joerg Halter, Dominik Heim, Yves Chalandon, Urs Schanz, Gayathri Nair, et al.

Transplantation and Cellular Therapy 000 (2023) 1–15

Transplantation and Cellular Therapy

journal homepage: www.astctjournal.org

ASTCT American Society for Transplantation and Cellular Therapy

Full Length Article
Analysis

Pharmacokinetic Modeling and Simulation with Pharmacogenetic Insights Support the Relevance of Therapeutic Drug Monitoring for Myeloablative Busulfan Dosing in Adult HSCT

Khalil Ben Hassine[1], Claire Seydoux[2], Sonia Khier[3,4], Youssef Daali[5,6], Michael Medinger[7], Joerg Halter[7], Dominik Heim[7], Yves Chalandon[8], Urs Schanz[9], Gayathri Nair[9], Nathan Cantoni[10], Jakob R. Passweg[7], Chakradhara Rao Satyanarayana Uppugunduri[1,#], Marc Ansari[1,11,#,*]

[1] *Department of Pediatrics, Gynecology and Obstetrics, Cansearch Research Platform for Pediatric Oncology and Hematology, Faculty of Medicine, University of Geneva, Geneva, Switzerland*
[2] *Division of Hematology, University Hospital of Basel, Basel, Switzerland*
[3] *Pharmacokinetic and Modeling Department, School of Pharmacy, Montpellier University, Montpellier, France*
[4] *Probabilities and Statistics Department, Institut Montpelliérain Alexander Grothendieck (IMAG), CNRS, UMR 5149, Inria, Montpellier University, Montpellier, France*
[5] *Division of Clinical Pharmacology and Toxicology, University Hospital of Geneva, Geneva, Switzerland*
[6] *Faculty of Medicine & Sciences, University of Geneva, Geneva, Switzerland*
[7] *Division of Hematology, University Hospital of Basel, Basel, Switzerland and University Basel, Basel, Switzerland*
[8] *Division of Hematology, Bone Marrow Transplant Unit, University Hospital of Geneva and Faculty of Medicine, University of Geneva, Geneva, Switzerland*
[9] *Department of Medical Oncology and Hematology, University Hospital of Zurich, Zurich, Switzerland*
[10] *Division of Oncology, Hematology and Transfusion Medicine, Kantonsspital Aarau, Aarau, Switzerland*
[11] *Division of Pediatric Oncology and Hematology, Department of Women, Child and Adolescent, University Geneva Hospitals, Geneva, Switzerland*

Article history:
Received 17 September 2023
Accepted 4 December 2023

Key Words:
Busulfan
Population pharmacokinetics
Physiologically-based pharmacokinetics

A B S T R A C T

Therapeutic drug monitoring (TDM) of busulfan (Bu) is well-established in pediatric hematopoietic stem cell transplantation (HSCT), but its use in adults is limited due to a lack of clear recommendations and scarcity of evidence regarding its utility. *GSTA1* promoter variants are reported to affect Bu clearance in both adults and pediatric patients. This study aimed to evaluate the value of preemptive genotyping *GSTA1* and body composition (obesity) in individualizing Bu dosing in adults, through pharmacokinetic (PK) modeling and simulations. A population pharmacokinetic (PopPK) model was developed and validated with data from 60 adults who underwent HSCT. Simulations assessed different dosing scenarios based on body size metrics and *GSTA1* genotypes. Due to the limited number of obese patients in the cohort, the effect of obesity on Bu pharmacokinetics

*Correspondence and reprint requests: Marc Ansari, Division of Pediatric Oncology and Hematology, Department of Women, Child, and Adolescent, University Hospital of Geneva, Rue Willy Donzé 6, 1211, Geneva, Switzerland.
E-mail address: Marc.Ansari@hcuge.ch (M. Ansari).
[#] These authors share last authorship.

https://doi.org/10.1016/j.jtct.2023.12.003

Therapeutic drug monitoring
Model-informed precision dosing
Limited sampling strategy
Hematopoietic stem cell transplantation

(PK) was evaluated *in silico* using a physiologically-based pharmacokinetic (PBPK) model and relevant virtual populations from Simcyp software. Patients with at least 1 *GSTA1*B* haplotype had 17% lower clearance on average. PopPK simulations indicated that adjusting doses based on genotype increased the probability of achieving the target exposure (3.7 to 5.5 mg.h/L) from 53% to 60 % in *GSTA1*A* homozygous patients, and from 50% to 61% in **B* carriers. Still, Approximately 40% of patients would not achieve this therapeutic window without TDM. A 2-sample optimal design was validated for routine model-based Bu first dose $AUC_{0-\infty}$ estimation, and the model was implemented in the Tucuxi user-friendly TDM software. PBPK simulations confirmed body surface area-based doses of 29 to 31 mg/m^2/6h as the most appropriate, regardless of obesity status. This study emphasizes the importance of individualized Bu dosing strategies in adults to achieve therapeutic targets. Preemptive genotyping alone may not have a significant clinical impact, and routine TDM may be necessary for optimal transplantation outcomes.

INTRODUCTION

Therapeutic drug monitoring (TDM) of busulfan (Bu) has been extensively studied and implemented in pediatric hematopoietic stem cell transplantation, allowing for personalized dosing based on clinical evidence that enabled to define therapeutic windows leading to optimal treatment outcomes [1–3]. However, in adults, despite the evidence suggesting exposure-response relationships in this population [4], there remains a scarcity of proper prospective evidence and clear recommendations for routine TDM of myeloablative conditioning (MAC) doses of Bu. A survey published in 2019 shows that only a minority of transplantation units perform TDM of MAC Bu for adult patients [5].

Bu has been recognized for its important inter-individual variability (IIV) in exposures, in relation to its narrow therapeutic window. That variability was partly explained by individual patients' characteristics such as patient body size, age (in pediatric patients), genetic [6], and more recently metabolomic markers [7]. *GSTA1* promoter polymorphisms, coding for glutathione-s-transferase A1 primarily involved in Bu metabolism, have been identified as factors contributing to the IIV in Bu PK and outcomes, both in adults [8–14] and pediatric patients [15–18]. In a multicenter randomized *BuCyBu* study (NCT01779882) conducted in adult patients undergoing HSCT for hematological malignancies in Switzerland, patients were randomized to receive cyclophosphamide either before or after Bu administration [19]. The comparison of noncompartmental analysis results suggested a higher exposure, in terms of first-dose AUC, in *GSTA1*B* haplotype carriers [8]. Nevertheless, it remained uncertain whether preemptive genotyping of *GSTA1* can be relevant for initial dosing adjustment in adult patients, serving as an alternative or a complement to routine TDM for individualizing Bu dosing and achieving the narrow therapeutic window in adult patients.

Using the data from the *BuCyBu* trial [4], the present study sought to assess the added value of preemptive genotyping and the role of body composition (obesity) in individualizing Bu dosing through model-based simulations.

The primary objective of this study was to develop a population pharmacokinetic (PopPK) model for Bu in adult patients and evaluate the impact of *GSTA1* promoter variants on Bu clearance (CL) IIV. By quantifying the extent of the genotype effect on Bu CL, we aimed to assess the potential value of incorporating preemptive genotyping into clinical practice for optimizing Bu dosing in adults. Using PopPK model-based simulations, we aimed to elucidate the potential benefits of individualizing Bu dosing based on *GSTA1* genotypes, and body size, and assess the necessity of routine TDM in adult patients. Different body size metrics were used for the simulations, to define an optimal dosing strategy regardless of their body composition of the patient. Because of the scarcity of obese patients in the studied cohort, we further developed a physiologically-based pharmacokinetic (PBPK) model to evaluate the impact of obesity on Bu pharmacokinetics, and define doses suitable for each patient.

METHODS

Patient Population

Adult patients (n = 60) from the study *BuCyBu* (NCT01779882) [4], for whom clinical, demographic, and PK data were available, were included in the present analysis. These patients

consented for their biological samples to be stored in the Swiss Transplant Cohort Study (SCTS) biobank and to be used for research purposes. DNA samples extracted from whole blood specimens were received upon approval (Application ID: FUP 151) by the SCTS Biobank scientific committee. The patients' DNA samples were genotyped for *GSTA1* promoter variants as previously described [20]. The clinical and demographic characteristics of the study cohort are described in Supplementary Material S1.

Bu Administration Protocol and PK Analyses

The treatment and PK analysis protocols were previously described [8,19]. The patients received 16 doses of Bu over 4 days (every 6-hour dosing). A 24-hour interval was maintained between the administration of Bu and Cy. Doses of 0.8 mg/kg actual body weight (ABW) were administered over 2 hours during the first day of Bu treatment, according to Bu's prescribing information [21]. The doses on the following days (from the fifth dose onwards) were adjusted using TDM results from the first dose, to achieve a per-dose exposure range of 3.7 to 5.5 mg.h/L (900 to 1350 μM.min). This range was selected to obtain a favorable balance between treatment efficacy and toxicity in adult patients [4,8,22]. Plasma concentration measurements were performed on samples withdrawn 2, 2.5, 3, 4, and 6 hours after the start of the first infusion. Following doses were modified by either increasing or reducing the dose by 25% in patients whose $AUC_{0\text{-}\infty}$ deviated from the target exposure range's bounds by more than 25%. No dose adjustments were performed for deviations of less than 25%. Bu TDM was conducted within each treating center, using a cross-validated analytical method to ensure Bu quantification accuracy and precision.

Population Pharmacokinetic Analysis

The PopPK model was developed in Phoenix NLME software (Certara, version 8.2) with the first-order conditional estimation and extended least squares (FOCE-ELS) method. The one and two-compartment models were explored as structural models, and the additive, proportional and mixed residual errors were tested for the statistical model. An exponential IIV was assumed for the PK parameters (log-normal distribution). Due to the availability of concentration data only from the first dose, interoccasion variability of the PK parameters was not estimated. The body weight of the patients was incorporated into the model using theoretical allometric scaling equations. Other derived body size metrics were not included in the model building process due to the absence of height data for 12 patients. A stepwise covariate screening was conducted using the Bayesian information criterion (BIC) as the objective function value, considering covariates in addition to body weight. The covariates tested on top of body weight were preconditioning levels of Aspartate Aminotransferase (ASAT), Alanine Aminotransferase (ALAT), Bilirubin, Albumin, the age of the patient, *GSTA1* genetics and the randomization group (Cy before Bu versus Bu before Cy). The model qualification included the assessment of goodness-of-fit plots, bootstrap re-estimation on 500 resampled datasets, and prediction-corrected visual predictive check plots with 1000 simulated replicates. These steps were undertaken to ensure the reliability and robustness of the developed model [23].

PopPK Model-Based Simulations

Considering the covariates of the 48 patients in our dataset for whom the height was available, we conducted Monte-Carlo simulations to generate 50 replicates for each patient. These simulations evaluated a range of single doses varying from 0.65 mg/kg to 1 mg/kg of ABW, ideal body weight (IBW), or adjusted ideal body weight at 25% fat (AIBW25) [24], as well as doses ranging from 25 to 39 mg/m^2 of body surface area (BSA) calculated with the Mosteller formula [25]. The adjusted body size metrics were calculated using the equations 1 to 4.

$$\text{Males: } \mathrm{IBW(kg)} = 50 + 0.91 \times (\mathrm{height(cm)} - 152) \quad (1)$$

$$\text{Females: } \mathrm{IBW(kg)} = 45 + 0.91 \times (\mathrm{height(cm)} - 152) \quad (2)$$

$$\mathrm{AIBW25\ (kg)} = \mathrm{IBW(kg)} + 0.25 \times (\mathrm{ABW(kg)} - \mathrm{IBW(kg)}) \quad (3)$$

$$\mathrm{BSA\ (m^2)} = \sqrt{\frac{\mathrm{ABW\ (kg)} \times \mathrm{height\ (cm)}}{3600}} \quad (4)$$

We also tested a dosing regimen based on ABW for individuals with BMI < 27 kg/m^2 and AIBW25 for BMI > 27 kg/m^2, as suggested by Nguyen et al. [24].

The outcome of interest was the probability of achievement of a first dose $AUC_{0\text{-}\infty}$ between 3.7 and 5.5 mg.h/L obtained with the different dosing scenarios, calculated as the proportion of simulated $AUC_{0\text{-}\infty}$ within the defined range. The

simulated AUC values were further stratified according to the *GSTA1* haplotype groups, allowing us to evaluate the potential of genotype-based initial dosing in reaching the targeted Bu exposures in adults.

Evaluation of Limited Sampling Strategy and Model Implementation in Tucuxi TDM Software

PFIM software 4.0 [26] with Fisher information matrix optimization using Federov-Wynn method was used for the determination of an optimal 2-sample design for TDM. The provided input time points for the selection of the optimal sampling timepoints were 0 h to 0.25 h to 0.5 h to 1 h to 4 h from infusion end. Once the optimal sampling schedule chosen, we tested the accuracy of model predictions of a single dose $AUC_{0-\infty}$ with limited samples compared to the Maximum *A Posteriori* (MAP) estimations with the extensive sampling used in the study. The model was then implemented in Tucuxi software [27] using the online drug file editor (available from: http://drugeditor.tucuxi.ch/) and a proficiency test was performed to assess the concordance between single doses $AUC_{0-\infty}$ obtained with Tucuxi and limited sampling, compared to those obtained with Phoenix software and full sampling.

PBPK Model Development

To evaluate the impact of obesity on Bu PK, a full-body PBPK model for Bu was developed using Simcyp software [28] (Certara, version 21). The construction of this model involved adapting a previously validated pediatric model (Ben Hassine, Khier et al., submitted manuscript) to the adult population. Drug-related parameters were obtained from literature sources, predicted using Simcyp models, or estimated based on observed data from the study population. A detailed overview of the drug-related parameters can be found in Table 1 [29–34].

Table 1
Summary of the PBPK Model Parameters Inputs

Parameter	Value	Source
MW	246.3 $g.mol^{-1}$	pubchem.ncbi.nlm.nih.gov [29]
Log P	-0.3	Diestelhorst et al. [34]
B:P	0.93	Dilo et al. [31]
fu_p	0.93	drugbank.ca [30]
fu_t	0.96	Simcyp predicted
K_p calculation method	Poulin and Theil with Berezhkovskiy modification	Berezhkovskiy et al. [32]
K_p scalar	1.10	Parameter estimation using study cohort and Diestelhorst et al. [34]
K_p liver	0.88	Simcyp predicted
K_p Adipose	0.21	Simcyp predicted
K_p Bone	0.53	Simcyp predicted
K_p Brain	0.94	Simcyp predicted
K_p Gut	0.84	Simcyp predicted
K_p Heart	0.87	Simcyp predicted
K_p Kidney	0.90	Simcyp predicted
K_p Lung	0.92	Simcyp predicted
K_p Muscle	0.87	Simcyp predicted
K_p Skin	0.83	Simcyp predicted
K_p Spleen	0.91	Simcyp predicted
K_p Pancreas	0.91	Simcyp predicted
K_m cytosolic enzyme	3680 μM	Bredschneider et al. [33]
V_{max} cytosolic enzyme	10,800 pmol/min/mg protein	Parameter estimation using study cohort.
% Extensive metabolizers (EM)	0.35	Study cohort (Supplementary Material S1)
% Poor metabolizers (PM)	0.65	Study cohort (Supplementary Material S1)
Relative abundance/activity of cytosolic enzymes in PM compared to EM	0.84	PopPK Bootstrap results (Table 2)

B:P indicates Blood:plasma partition ratio; fu_p: Fraction unbound in plasma; fu_t: Fraction unbound in tissue; K_m: Michaelis constant; K_p: Tissue:plasma partition coefficient; MW: Molecular weight; V_{max}: maximum reaction velocity.

Considering that less than 2% of Bu is eliminated unchanged in urine [6], it was assumed that the entire elimination of Bu occurs through hepatic metabolism. The reported K_M value for Bu conjugation with cytosolic enzymes responsible for its metabolization, as previously described by Bredschneider et al. [33], was incorporated in the model. However, due to the inadequacy of the reported in vitro V_{max} values in describing the observed clearance (CL) in patients, the V_{max} value was estimated through parameter estimation using the observed data. The fraction of Bu unbound to microsomes was assumed to be equivalent to the unbound fraction in the tissue. The amount of glutathione (cofactor) available for Bu conjugation was assumed to be in excess, and not impacting the metabolization kinetics [35].

For Monte Carlo simulations and comparison of PK exposure parameters, 3 different Simcyp virtual populations were utilized: obese, healthy adults, and cancer populations. The physiological parameters of the adult cancer population were assumed to be similar to those of the patient population under investigation. Single-dose simulations of 0.8 mg/kg ABW infused over 2 hours, were conducted on 10 virtual cohorts, each comprising 10 patients (totaling 100 virtual patients for each population). The model simulations with the virtual cancer population were validated against observed data from our cohort, with a comparison of observed versus simulated concentrations, as well as the area under the concentration-time curve ($AUC_{0-\infty}$) determined using MAP, and the observed maximum concentration (C_{max}). A geometric mean fold error (*GMFE*), defined as the geometric mean of simulated parameters divided by the geometric mean of observed parameters, falling within the range of 0.8 to 1.25, was used as the criterion for PBPK model validation. Visual assessment of the concordance between observed and simulated concentrations was also performed. Local sensitivity analyses were performed on different organ volume scalars (liver, adipose, and plasma) and cardiac blood output to evaluate their influence on the disposition of Bu and understand the effect of obesity on Bu pharmacokinetics.

Further simulations were conducted using doses of 31 or 29 mg/m^2 BSA to explore the potential of BSA-based dosing in mitigating obesity-related difference in exposure. After the evaluation of single doses, Multiple doses simulations regimens were performed, with a focus on 4 times daily dosing (q6h, every 6 hours), and once daily dosing (q24h, every 24 hours).

RESULTS

PopPK Model Development and Validation

The dataset included 296 measured Bu plasma concentrations, none of them being below the limit of quantification of the analytical methods. Four concentrations from 4 patients were missing. A two-compartment model with linear elimination, zero-order infusion rate and proportional residual error was the most adequate structural model to describe our PK data. The model was macro-parametrized in terms of systemic CL, intercompartmental clearance (Q), Volumes of distribution of the central compartment (V_c) and peripheral compartment (V_p). V_p and its random variability could not be precisely estimated. V_p was therefore estimated as a factor of V_c. The theoretical allometry of bodyweight for CL, V_c and Q improved the BIC by 29.52 units compared to the structural model. An exploration of covariate effects was performed. The plots of individual deviations from the population value of parameters (ETA) (Supplementary Material S2) suggested a significantly lower CL in *GSTA1*B* haplotype carriers (Mann-Whitney test $P = .0097$), while a trend of increased CL was observed in patients who received Cy before Bu (Mann-Whitney test $P = .0611$). Other continuous covariates did not show any trend or correlation with the PK parameters' ETAs (Supplementary Material S2). In stepwise covariate modeling (Supplementary Material S3), only *GSTA1* genetics (**A*A* versus **A*B* and **B*B*) significantly decreased the objective function value (Δ BIC = - 5.6, Δ IIV CL = -14 %). The final model parameters and the bootstrap estimations are presented in Table 2. The final model estimates suggest that Bu CL was 17% lower in patients carrying at least 1 **B* haplotype (65% of the study population). The final model parameters all fell within the 95% confidence intervals of the bootstrap estimates. The diagnostic plots were adequate (Figure 1A-D) and showed a good concordance between observed and model predicted values, and a homogeneous distribution of the conditional weighted residuals around the identity line. The VPC plots (Figure 1E-H) displayed an acceptable correspondence between simulated and observed values, even when the analysis was stratified by *GSTA1* haplotype. A shrinkage of 25% for the IIV of Q was accepted as it was below the critical threshold of 30% [36].

PopPK Model-Based Simulations

The simulation results of the first dose $AUC_{0-\infty}$ are displayed in Figure 2, and the simulations-based probabilities of target achievements are

Table 2
Model Final and Bootstrap Estimates

Parameters	Final Estimate (RSE %)	Shrinkage	500 Bootstraps (95% CI)
Fixed effects			
tvCL in CL = tvCL × $(ABW/70)^{0.75}$	13.89 (3)		13.88 (12.89-14.63)
tvVc in Vc = tvVc × ABW/70	29.80 (8)		29.58 (23.79-33.84)
tvQ in Q = tvQ × $(ABW/70)^{0.75}$	27.74 (26)		30.73 (16.88-63.94)
tvVp in Vp = tvVp × Vc	0.61 (17)		0.61 (0.47-1.01)
GSTA1 *B covariate effect on CL	−0.17 (19)		−0.16 (-0.23 to -0.07)
Random effects			
IIV CL	23 (18)	0.03	23 (11-35)
IIV Vc	21 (32)	0.07	20 (11-29)
CL-Vc correlation	0.58		0.59
IIV Q	75 (30)	0.25	84 (31-137)
Residual error			
proportional	0.06 (8)	0.19	0.06 (0.05-0.07)

CL indicates clearance; IIV: Inter-individual variability; Q: Intercompartment clearance; tv: typical value; Vc: central volume of distribution; Vp: peripheral volume of distribution.

displayed in Table 3. On the unstratified population, the currently recommended doses ie, 0.8 mg/kg, was the one maximizing the probability of target achievement (57%). However, when the population is stratified by their *GSTA1* haplotype, this conventional dosing resulted in important overexposure among patient harboring at least one **B* haplotype, and underexposure in **A* homozygous patients. The most adequate ABW-based dosage for **A* homozygous patients was 0.9 mg/kg as it increased the probability of target achievement from 53 % to 60 % in this stratum, whereas for **B* carriers, a dose of 0.75 mg/kg increased the probability of target achievement from 58 % to 61 %. BSA based dosing (31 mg/m^2) enables to achieve similar probabilities of target achievements than ABW base dosing, and similar trends were observed when adapting the doses to the genotypes. A dose of 35 mg/m^2 increased the probability of target achievement from 57 % to 61 % in **A* homozygous patients, and a dose of 29 mg/m^2 increased this probability from 57% to 60%

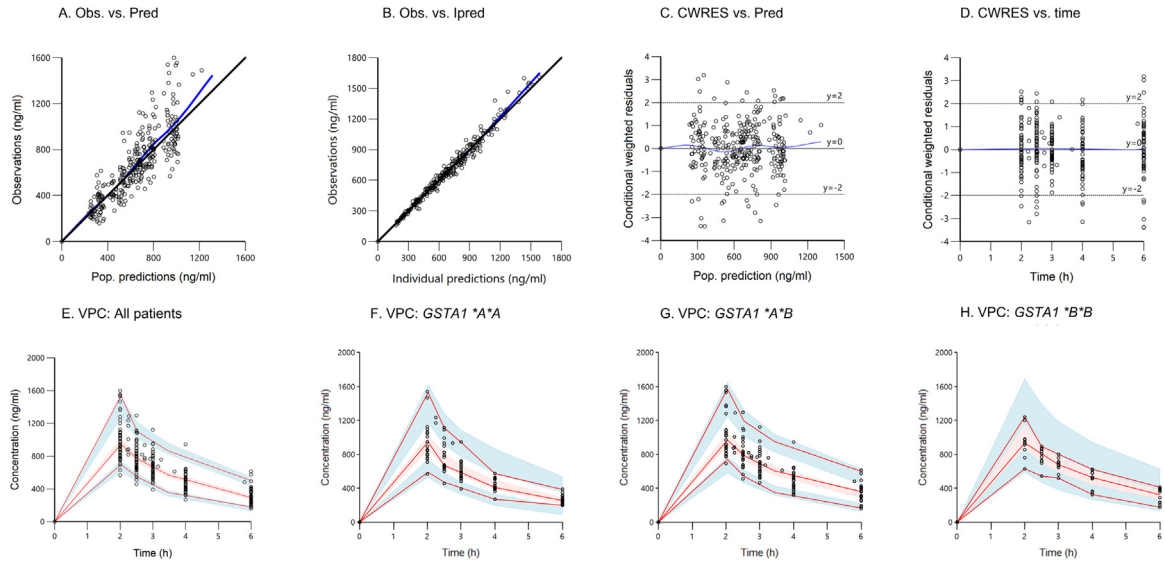

Figure 1. Goodness-of-fit plots (A-D) and visual predictive checks (VPC, E-H) for PopPK model qualification. In plots A-B, the black solid lines represent identity lines, the blue solid lines represent the Loess regression. In the plots E to H, the shaded areas represent the 95% confidence intervals of the simulations' 5th, 50th, and 95th percentiles. The red lines represent the 5th, 50th, and 95th observed percentiles. The black dots represent the observed concentrations. Plots F to H are from VPC stratified by GSTA1 haplotypes.

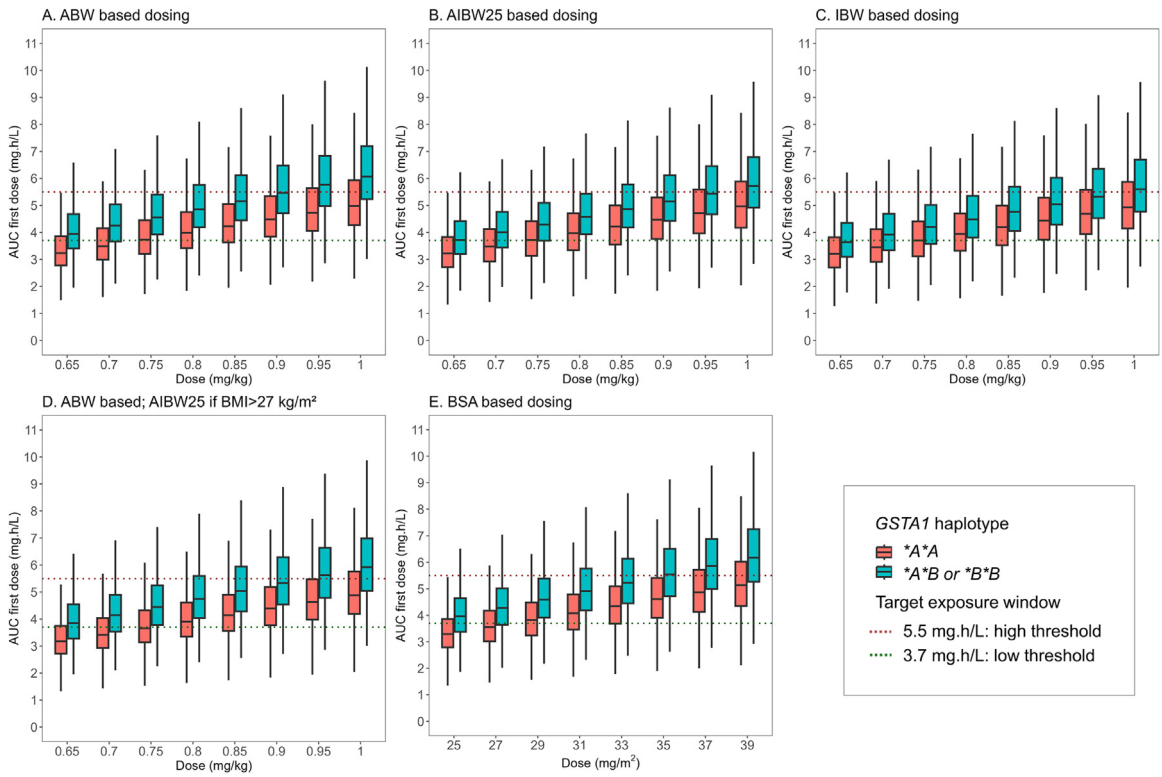

Figure 2. PopPK based simulations of dosing based on different body size metrics. ABW: Actual bodyweight; AIBW, Adjusted ideal bodyweight; IBW: Ideal bodyweight; BSA: Body surface area.

in **B* carriers. Nevertheless, using the different body size metrics and even with doses adjusted to the genotype of the patients, at least 39 % of the patients are not predicted to achieve the targeted exposure, highlighting the need for TDM-based dose adjustments to harmonize the exposures among patients.

Limited Sampling Strategy Evaluation and Model Implementation in Tucuxi

Because we showed in the previous part that TDM of Bu is necessary for the achievement of the target of 3.7 to 5.5 mg.h/L, we tested a limited sampling strategy to facilitate the implementation of routine TDM. A 2-sample TDM design was proposed by PFIM software, with samples taken at peak and trough concentrations (at the end and 4 hours after the end of infusion). The plots in Supplementary Material S4 show a very good concordance between the $AUC_{0-\infty}$ predicted with limited sampling in tucuxi software, compared to full sampling (Linear regression: R^2 = 0.9772; Bland-Altman: 95% limits of agreement: -7.98% to 6.49%), confirming the suitability of Tucuxi software for PK parameter estimation with limited sets of samples.

PBPK Model Simulations

One of the challenges in our study cohort was the scarcity of obesity in the dataset (only 1 patient with BMI >30 kg/m^2, Supplementary Material S1) making it difficult to evaluate dosing strategies in obese patients. For this reason, we attempted to explore dosing regimens that are suitable for both obese and nonobese patients using relevant virtual populations in Simcyp software, while exploring physiological and PK differences between the different virtual populations. The model simulations in the cancer population showed an adequate concordance with simulated concentrations (Figure 3A). Nonetheless, a higher variability around the peak concentration could not be entirely described by the model. The *GMFE* of $AUC_{0-\infty}$ was 0.92 and the *GMFE* of C_{max} was 1.04, both results being within the acceptable range of 0.80 to 1.25. The PBPK model was thus validated and ready to be used for further simulations. The simulations with 0.8 mg/kg ABW showed a higher exposure in the obese population compared to both cancer and healthy population (Figure 3B and C). Table 4 shows the difference in relevant demographic, physiological and exposure parameters between the three tested virtual populations. Despite a higher predicted Bu systemic

Table 3
PopPK Simulation-Based Probability of Target Exposure Achievement ($AUC_{0-\infty}$ first dose 3.7 to 5.5 mg.h/L) with Different Body-Size Based Dosing Regimens

		Probability of Target Achievement		
Body Size Descriptor	Dose	Overall	*A*A	*A*B/*B*B
Actual bodyweight (ABW)	0.65 mg/kg	45%	29%	54%
	0.70 mg/kg	51%	38%	59%
	0.75 mg/kg	56%	47%	61%
	0.80 mg/kg	57%	53%	58%
	0.85 mg/kg	55%	57%	53%
	0.90 mg/kg	52%	60%	47%
	0.95 mg/kg	45%	57%	39%
	1.00 mg/kg	40%	56%	31%
25% Adjusted bodyweight (AIBW25)	0.65 mg/kg	39%	28%	46%
	0.70 mg/kg	48%	37%	54%
	0.75 mg/kg	54%	46%	59%
	0.80 mg/kg	57%	53%	59%
	0.85 mg/kg	57%	56%	58%
	0.90 mg/kg	55%	58%	54%
	0.95 mg/kg	51%	57%	47%
	1.00 mg/kg	46%	56%	40%
Ideal bodyweight (IBW)	0.65 mg/kg	37%	28%	43%
	0.70 mg/kg	45%	36%	51%
	0.75 mg/kg	51%	45%	55%
	0.80 mg/kg	55%	50%	58%
	0.85 mg/kg	57%	55%	58%
	0.90 mg/kg	55%	55%	54%
	0.95 mg/kg	51%	54%	49%
	1.00 mg/kg	46%	53%	43%
ABW, or AIBW25 if BMI > 27	0.65 mg/kg	41%	25%	50%
	0.70 mg/kg	48%	34%	56%
	0.75 mg/kg	54%	45%	60%
	0.80 mg/kg	56%	52%	59%
	0.85 mg/kg	56%	56%	55%
	0.90 mg/kg	54%	59%	51%
	0.95 mg/kg	49%	59%	43%
	1.00 mg/kg	44%	59%	35%
Body surface area (BSA)	25 mg/m^2	44%	30%	52%
	27 mg/m^2	52%	40%	59%
	29 mg/m^2	56%	50%	60%
	31 mg/m^2	57%	57%	58%
	33 mg/m^2	55%	59%	53%
	35 mg/m^2	51%	61%	45%
	37 mg/m^2	45%	59%	38%
	39 mg/m^2	39%	55%	30%

CL in obese patients, probably resulting from an observed higher liver volume, and higher liver arterial and portal blood flows due to a higher cardiac output in obese patients, the obese population displays a mean $AUC_{0-\infty}$ that is 16 % higher than that of cancer population and 29 % higher than healthy population, which is paradoxical given the known relationship between AUC, dose and clearance ($AUC_{0-\infty}$ = Dose/CL). However, the obese population displays a lower steady-state volume of distribution (V_{ss}) which is responsible the higher observed exposure and peak

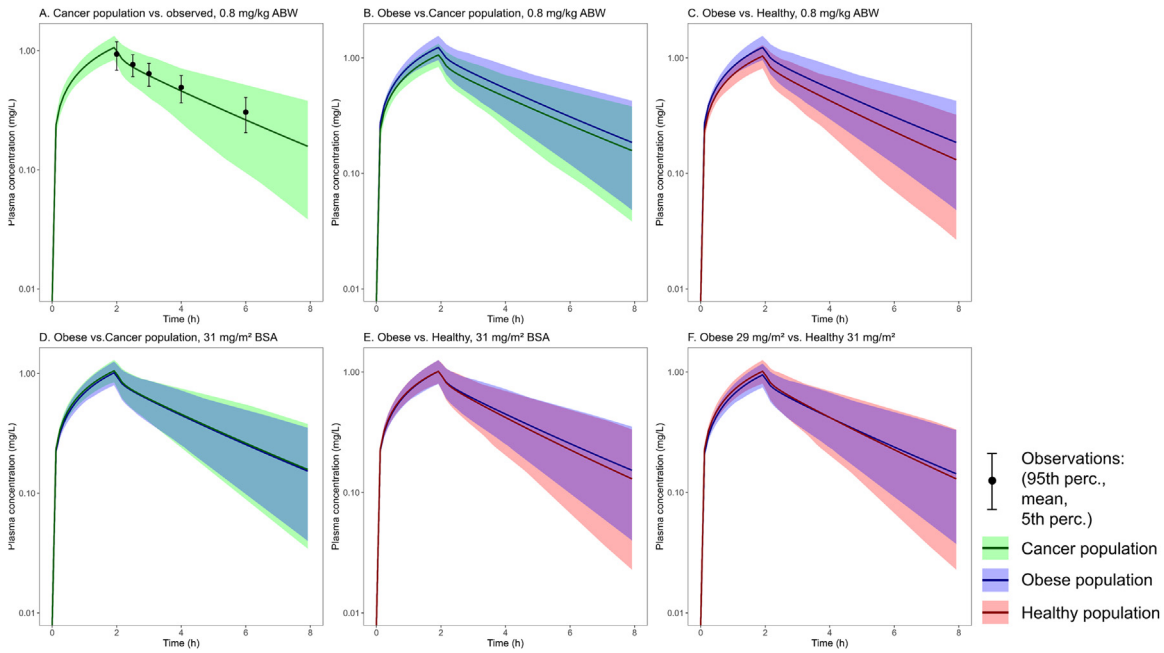

Figure 3. PBPK simulations of actual bodyweight (ABW) and body surface area (BSA) single dosing in healthy, obese and cancer Simcyp populations. The solid lines represent the mean concentrations, while the shaded areas represent the range between the 5th and 95th percentiles.

concentrations in those patients. Several factors could explain this lower V_{ss}. According to the results in Table 4, this lower V_{ss} is possibly due to the increased adipose tissue volume in the virtual obese population. This was accompanied by a predicted higher AUC in the adipose tissue. A redistribution from the adipose compartment to the systemic circulation could explain the increase exposures in obese patients. The sensitivity analysis results in Supplementary Material S5 shows that the AUC maintains a relative stability with increasing body weight when dosing is based on BSA. Nevertheless, there is a drastic AUC increase with body weight, when 0.8/mg/kg ABW-based doses are simulated. Increasing adipocyte tissue volume scalar, in the cancer virtual population, decreases V_{ss} while CL is unchanged, explaining the increase exposure in obese population. When using a dose of 31 mg/m^2, instead 0.8 mg/kg ABW, the difference in exposure attributed to obesity was remarkably reduced (Figure 3D and E, Table 4). A slightly reduced dose of 29 mg/m^2 in the obese population further diminished the difference in exposure with the healthy virtual population (Figure 3F, Table 4). Our simulations suggest that BSA-based dosing achieves comparable Bu exposure levels in both obese and nonobese patients.

Table 5 shows the simulated parameters with multiple BSA-based dosing, for q6h and q24h regimens, both with PBPK and PopPK modeling. Both models resulted in similar simulated values for C_{max} and $AUC_{0\text{-}\infty}$. Consistently with the known first-order elimination of Bu, the cumulative $AUC_{0\text{-}\infty}$ was very similar (Identical in PopPK simulations) between q6h and q24h dosing. Approximately 3 times higher peak concentrations where obtained when 4 times the q6h dose of Bu is given once a day.

DISCUSSION

Our study aimed to propose personalized dosing strategies of busulfan (Bu) for adult patients, conducting top-down and bottom-up PK model-based simulations. We evaluated different dosing scenarios based on body size metrics and *GSTA1* genotype with the aim of improving the therapeutic window targeting. To further explore Bu dosing strategies in the obese population, we employed a physiologically-based pharmacokinetic (PBPK) model.

Consistent with our previous findings [8], the presence of the *GSTA1*B* haplotype had a significant impact on Bu clearance. Through the population approach, we were able to quantify this effect, revealing an average of 17% decrease in clearance (CL) in *GSTA1*B* carriers. We tested 2 haplotyping strategies in our covariate analysis: 1 based on the single nucleotide polymorphism -69C/T rs3957357 (**A* and **B* haplotypes) and the other using a grouping based on 6 SNPs of the promoter haplotype (**A1, *A2, *B1a*, etc.), as

Table 4
Results of Single Dose PBPK Model Simulations with Different Virtual Population

		Virtual Cancer	Virtual Obese	Virtual Healthy	*In Vivo* Cohort (Observed)
BMI (kg/m^2)		24.1 (19.3-33.3)	34.6 (31.5-38.1)	24.6 (19.7-34.3)	23.1 (18.4-28.16)
% BMI $\geq$ 30 kg/m^2 (Obesity class I and above)		12%	100%	14%	2%
Liver volume (L)		1.5 (1.2-1.9)	1.7 (1.3-2.2)	1.5 (1.1-2.0)	
Liver blood flow arterial (L/h)		18.6 (15.5-22.1)	19.7 (16.3-23.5)	21.5 (17.2-26.6)	
Liver blood flow portal (L/h)		57.1 (46.7-67.1)	59.6 (52.7-71.9)	66.7 (54.6-80.08)	
Adipose tissue volume (L)		17.7 (3.7-44.8)	42.3 (21.6-61.2)	20.2 (4.5-46.0)	
Adipose tissue blood flow (L/h)		16.3 (12.4-24.9)	34.7 (29.4-54.2)	19.7 (14.7-30.1)	
Plasma volume (L)		3.7 (2.7-5.9)	3.5 (2.6-4.9)	3.1 (2.4-4.5)	
Erythrocytes volume (L)		1.6 (1.1-2.3)	2.1 (1.3-2.8)	1.8 (1.2-2.6)	
Hematocrit (%)		36.4 (29.7-45.5)	40.5 (35.0-46.9)	40.5 (35.2-47.2)	
Serum albumin (g/L)		39.0 (29.2-49.3)	44.7 (38.0-51.1)	46.3 (39.8-52.3)	
V_{ss} (L/kg)		0.58 (0.45-0.71)	0.48 (0.41-0.58)	0.56 (0.44-0.68)	
Dose: 0.8 mg/kg ABW	Plasma $AUC_{0-\infty}$ (mg.h/L)	4.22 (2.63-7.75)	4.91 (3.03-8.64)	3.81 (2.36-7.02)	4.48 (3.10-6.65)
	Plasma C_{max} (mg/L)	1.06 (0.85-1.37)	1.27 (0.98-1.59)	1.04 (0.83-1.33)	0.98 (0.75-1.49)
	Systemic CL (L/h)	14.28 (6.90-22.88)	16.26 (8.80-28.38)	15.27 (7.86-26.32)	12.46 (8.09-21.30)
	Mean liver $AUC_{0-\infty}$ (mg.h/L)	3.21	3.65	2.96	
	Mean liver C_{max} (mg/L)	0.75	0.84	0.74	
	Mean adipose $AUC_{0-\infty}$(mg.h/L)	0.95	1.10	0.86	
	Mean adipose C_{max} (mg/L)	0.22	0.25	0.21	
Dose: 31 mg/m^2 BSA	Plasma $AUC_{0-\infty}$ (mg.h/L)	4.42 (2.55-7.92)	4.27 (2.50-7.08)	4.00 (2.28-7.08)	
	Plasma C_{max} (mg/L)	1.08 (0.86-1.33)	1.04 (0.81-1.29)	1.04 (0.81-1.29)	
	Systemic CL (L/h)	14.28 (6.90-22.88)	17.24 (8.80-28.38)	15.27 (7.86-26.32)	
	Mean liver $AUC_{0-\infty}$ (mg.h/L)	3.20	3.00	2.90	
	Mean liver C_{max} (mg/L)	0.75	0.69	0.72	
	Mean adipose $AUC_{0-\infty}$(mg.h/L)	0.94	0.91	0.85	
	Mean adipose C_{max} (mg/L)	0.21	0.20	0.20	
Dose: 29 mg/m^2 BSA	Plasma $AUC_{0-\infty}$ (mg.h/L)	4.13 (2.38-7.41)	4.00 (2.33-6.71)	3.74 (2.13-6.63)	
	Plasma C_{max} (mg/L)	1.01 (0.80-1.24)	0.97 (0.76-1.21)	0.97 (0.76-1.21)	
	Systemic CL (L/h)	14.28 (6.90-22.88)	17.24 (8.80-28.39)	15.27 (7.86-26.33)	
	Mean liver $AUC_{0-\infty}$ (mg.h/L)	3.00	2.81	2.72	
	Mean liver C_{max} (mg/L)	0.70	0.65	0.67	
	Mean adipose $AUC_{0-\infty}$(mg.h/L)	0.89	0.85	0.79	
	Mean adipose C_{max} (mg/L)	0.20	0.19	0.19	

The results are presented in terms of mean with 5th and 95th percentiles, unless differently indicated. *In vivo* $AUC_{0-\infty}$, C_{max}, and CL were generated with *Post hoc* individual parameter estimation from the developed PopPK model.
ABW indicates Actual body weight, BMI: Body mass index; BSA: Body surface area; V_{ss}: steady-state volume of distribution.

Table 5
Multiple Doses Simulations with 31 mg/m^2/6h for 4 Days of Treatment (Myeloablative Conditioning) with the Developed PopPK and PBPK Models

	q6h: 31 mg/m^2 in 2 h Infusion Per Dose, 16 doses		q24h: 124 mg/m^2 in 3 h Infusion Per Dose, 4 Doses	
	$cAUC_{0-\infty}$ (mg.h/L)	$C_{max,ss}$ (mg/L)	$cAUC_{0-\infty}$ (mg.h/L)	$C_{max,ss}$ (mg/L)
PopPK	75.72 (49.26-110.64)	1.26 (0.90-1.92)	75.72 (49.26-110.64)	3.69 (2.46-4.91)
PBPK (Cancer population)	70.68 (40.92-126.20)	1.28 (0.92-1.95)	70.85 (40.94-127.11)	3.58 (2.70-4.59)

The results are presented as mean with 5th and 95th percentiles.
$cAUC_{0-\infty}$ indicates cumulative area under the curve; $C_{max,ss}$: peak concentrations at steady state.

previously described by our group, better explained the IIV in Bu CL among pediatric patients [15]. This might be attributed to the low frequency (7%) of rapid metabolizer in this adult cohort (Supplementary Material S1). The present analysis showed that the single SNP grouping was more appropriate in this adult cohort. Furthermore, we observed no difference in clearance between **B* heterozygous and homozygous patients, indicating that the presence of at least 1 **B* haplotype decreased clearance to the same extent as **B* homozygosity. Similar findings were reported by Choi et al. [14], who found a 15% decrease in Bu clearance associated with this haplotype in a cohort of Korean adult patients with various malignant disorders. This altered relationships between genotype and phenotype in adults and pediatric patients necessitate further investigation in future studies. More recently, a pharmacometabolomic analysis by McCune et al. showed that a multiple linear regression including 13 endogenous metabolomic compounds tested 2 weeks before Bu dose, along with patient sex, explained 40% of the variation in Bu CL [7]. Whether these metabolomic compounds could further optimize Bu precision dosing for adults remain to be evaluated.

PopPK simulations revealed a modest increase in the probability of achieving therapeutic target levels after dose adjustment to the *GSTA1* genotype, making preemptive genotyping unlikely to be clinically impactful in adult patients. Our simulations indicated that even with adjustment according to *GSTA1* genotype, approximately 40% of patients would still fail to achieve the therapeutic target exposure range of 3.7 to 5.5 mg.h/L, due to a remaining unexplained PK variability. Moreover, incorporating different body size metrics into the simulations did not improve the proportion of individuals reaching target window. Nguyen et al. [24] suggested adjusted body size metrics such as adjusted ideal body weight at 25% (AIBW25) for patients with a BMI above 27 kg/m^2 or body surface area (BSA) as the most appropriate metrics for Bu dose calculation in adult patients. Our results showed that BSA-based dosing results in similar probability of target achievement compared to ABW-based dosing, suggesting its utility for nonobese adults, as there is only 1 obese individual in our cohort (Figure 1, Table 3).

The PBPK model enabled us to further explore Bu dosing strategies for obese patients. BSA based dosing resulted in similar exposures in obese and nonobese virtual populations (Figure 3E and F). Doses of 29 to 31 mg/m^2 are appropriate for all patients, regardless of their BMI. This is in line with Nguyen et al. simulation results suggesting that a dose of 29 mg/m^2 resulted in appropriate achievement of target exposure and enable to achieve similar exposures compared to AIBW25 based dosing [24]. AIBW25 based dosing in the PBPK simulations was not performed due to the unavailability of this metric in the software.

Bu doses are commonly adjusted in the case of obesity among adult patients. Recent surveys indicate that the majority of transplantation centers utilize adjusted ideal body weight at 25% (AIBW25) for Bu dosing in obese adult patients, typically at a dose of 0.8 mg/kg AIBW25, and ABW is employed for dosing in nonobese patients [5], as recommended by the EMA summary of product characteristics [21] and FDA prescribing information [37]. Other strategies reported in these surveys are the use of ideal body weight (IBW), or a body weight with 40% body fat adjustment (AIBW40) [5]. The categorization of obese patients also varies among centers, predominantly based on BMI or weight above IBW. Surprisingly, 25% of the centers surveyed do not adjust Bu doses in obese patients [5].

According to our PBPK simulations, ABW based dosing in obese patients results in higher exposures and may potentially lead to increased risks of treatment related adverse events. In accordance

with this finding, The American Society of Bone Marrow Transplantation (ASBMT) suggest the use AIBW25 for both obese and nonobese patients [22,38]. A study in adults with hematological malignancies reported that IBW-based dosing resulted in a larger proportion of subtherapeutic exposures, and lower progression-free survival in obese patients [39]. The former highlights the limitation of the use of body weight adjustment, which could lead to under dosing the patients and result in subtherapeutic exposure and treatment inefficacy, especially when TDM is not performed. Notably, the body surface area (BSA)-based strategy proposed by Nguyen et al. [24] is not used at all, as indicated by the aforementioned surveys [5]. This approach yields equivalent exposures between obese and nonobese populations, addressing the concerns associated with ABW-based dosing in obese patients. Consequently, adopting a fixed BSA-based dosing strategy is supported by our findings and offers a promising alternative for optimizing Bu dosing in all patients, regardless of their obesity status (Table 3, Figure 2E, Figure 3D and E).

Multiple studies have highlighted the relationship between Bu exposure and various clinical outcomes, such as event-free survival, overall survival, treatment-related toxicities, and mortalities [40–44]. Despite this, there is still a scarcity of evidence from well-designed prospective randomized studies that strongly support the superiority of therapeutic drug monitoring (TDM) guided Bu dosing in the adult population [5]. In a randomized study conducted by Andersson et al., the superiority of TDM guided Bu over fixed dosing was demonstrated. This approach resulted in lower relapse risk, lower treatment-related mortality, and significantly improved overall survival and event-free survival compared to fixed doses of 130 mg/m^2/day (32.5 mg/m^2/6h) [45]. Nevertheless, further studies of similar nature are required to justify the widespread adoption of Bu TDM in adults. A recent meta-analysis conducted by Chen et al. not only revealed that TDM-guided Bu is more effective and safer, but also highlighted its cost-effectiveness compared to fixed dosing [46]. However, the survey by Ruutu et al. reported that only a small percentage of EBMT reporting transplantations centers perform TDM in Bu MAC conditioning [5]. This can be attributed to the lack of clear recommendations and the limited evidence demonstrating the superiority of TDM-guided Bu dosing in adults [22]. Other possible explanations could be the difficulty of TDM due to limited of access to TDM laboratories, or the lack of expertise for PK estimation and interpretation. Hence, we established an LSS for accurate model-based estimation AUC using only two sampling time points, and implemented the model to a user-friendly software, which could facilitate the feasibility of Bu TDM. Bu's Dose individualization based on the TDM of test doses have been highlighted as advantageous in terms of therapeutic target achievement and reduction of exposure variability, compared to weight-based dosing [47,48]. Model-based Bayesian forecasting with LSS is also useful for the accurate estimation of the PK parameters of test-doses, while avoiding extensive sampling [49]. Our model can be used for that purpose with the help of the user-friendly TDM software and the validated limited sampling strategy.

In the review and position statement of the ASBMT, it was stated that dosing regimens of Bu requiring 12 mg/kg *per-os* equivalent are recommended to have "PK targeting as appropriate for the disease state" [38]. Bu regimens with myeloablative doses fall within this category. However, this recommendation does not clearly specify when and how this "PK targeting" should be performed. In the more recent recommendation paper from the same society, no clear recommendation was issued for TDM in MAC regimens. Nonetheless, the TDM for reduced intensity regimens was considered not necessary [22], as it was stated that TDM is considered only for high dose Bu, and when the regimen was developed with BU TDM. The lack of clear recommendation could be due to the heterogeneity of the published studies and their small sample sizes [22]. Interestingly, The "Société Francophone de Greffe de Moelle et Thérapie Cellulaire" (SFGM-TC) recommends Bu TDM for adults, if Bu is administered orally, in case of severe hepatic impairment, in obese patients (BMI$>$ 30 kg/m^2), or in second allogeneic transplantations [50]. Overall, while some studies have indicated the benefits of TDM-guided Bu dosing, there is a need for more extensive research and well-designed prospective studies to establish its superiority and guide clinical practice recommendations effectively. Our study supports the relevance of TDM of MAC Bu at least for exposure target attainment. Whether a better targeting of the therapeutic window will be translated into improved outcomes remains to be further proved, despite the current evidence [45].

As previously mentioned, the study had a limitation due to the small number of obese patients included. Given the growing prevalence of obesity in several countries, we recognized the

importance of exploring this aspect, even in the absence of in vivo data. Therefore, we conducted an *in-silico* evaluation of Bu dosing for obesity using the physiological parameters of the virtual populations of the Simcyp software. It would be beneficial to prospectively evaluate the BSA-based dosing strategy coupled with TDM. Another limitation of the study was the lack of measurements of Bu concentrations in multiple dosing occasions, which hindered the analysis of inter-occasion variability. In a study by Langenhorst et al. [51], the authors developed a semimechanistic model to understand the dynamics of glutathione depletion in adult patients, the significance of which increased with age after 40 years of age. This inter-occasion variability may require TDM on multiple occasions to ensure an accurate targeting of cumulative exposures. It is worth noting that the glutathione reservoir may also differ between obese and nonobese populations [52], although this aspect was not evaluated in the present analysis.

CONCLUSIONS

In conclusion, this analysis confirmed the impact of *GSTA1* variants on Bu CL. The potential clinical impact of the adjustment of the starting dose to the *GSTA1* genotype of the patient seems to be modest. BSA based dosing (29 to 31 mg/m^2/6h) can be reliably applied in all patients, regardless of their body mass index. Our study shows the importance of TDM in achieving the therapeutic target AUC window of 3.7 to 5.5 mg.h/L. We hypothesize that TDM could have an important clinical impact in adult HSCT, despite its acrace utilization in these patients. Further randomized studies should assess the clinical utility of TDM-based dose adjustments compared to fixed dosing. The findings from this study may have important implications for improving therapeutic outcomes, and minimizing the risk of toxicity and nonrelapse mortality in adult patients undergoing HSCT with myeloablative (MAC) Bu conditioning treatment. The routine implementation of TDM for MAC Bu conditioning has the potential to optimize drug exposure, and ultimately improve and harmonize patients' outcomes.

DATA AVAILABILITY

The patients' data analyzed in this study is available from the corresponding author upon reasonable request, and ethics committee clearance. The simulated data, and Tucuxi drug file are available upon request from the corresponding author.

ACKNOWLEDGEMENTS

We thank Dr. Simona Mlakar and Mme. Mary Boudal-Khoshbeen for helping us with the genotyping of GSTA1 promoter SNPs. We also thank Dr. Tiago Nava for his help in organization of the pharmacogenomic part of the study for STCS submission. We express our gratitude for the help in DNA sample shipment and organization by Mr. Denis Marino from CANSEARCH Research platform on pediatric oncology and hematology and Mme. Simona Rossi from biobank of STCS. We acknowledge the CANSEARCH foundation for the financial support.

Financial disclosure: This work was financially supported by Baxter SA and Robapharm/Pierre Fabre SA and the CANSEARCH foundation.

Conflict of interest statement: None to declare related to the present work.

Independently from this work: YC has received honoraria for participation in symposia and advisory boards from MSD, Novartis, Incyte, BMS, Pfizer, Abbvie, Roche, Jazz, Gilead, Amgen, AstraZeneca, Servier; Travel support from MSD, Roche, Gilead, Amgen, Incyte, Abbvie, Janssen, AstraZeneca, Jazz, Sanofi, all via the institution. MA has received travel support from Jazz

Authorship statement: KBH: Design and conceptualization of the analysis, Development and application of the PopPK modeling and simulation scripts and workflow, development and validation of the PBPK model, PBPK model simulations, data interpretation, manuscript draft and revision. CS: Design, conduction and administration of the initial clinical trial, clinical and PK data curation, manuscript revision. SK: Development of the PBPK model, manuscript revision. YD: PK analyses, PK data curation, Provided PBPK modeling software, manuscript revision. MM: Design and conduction of the initial clinical trial, manuscript revision. JH, DH, YC, US, GN, NC: Performed the initial clinical trial, manuscript revision. JRP: Design, conduction and administration of the initial clinical trial, Study clinical data curation, manuscript revision. CRSU: Conceptualization of the analysis, PK data curation and analyses, PGx analyses, data interpretation, manuscript revision. MA: Conceptualization of the analysis, data analysis and interpretation, project administration, manuscript revision.

SUPPLEMENTARY MATERIALS

Supplementary material associated with this article can be found in the online version at doi:10.1016/j.jtct.2023.12.003.

REFERENCES

1. van der Stoep MYEC, Oostenbrink LVE, Bredius RGM, et al. Therapeutic drug monitoring of conditioning agents in pediatric allogeneic stem cell transplantation; where do we stand? *Front Pharmacol*. 2022;13:826004. Available at: https://www.frontiersin.org/articles/10.3389/fphar.2022.826004. Accessed June 23, 2023.
2. Ben Hassine K, Powys M, Svec P, et al. Total body irradiation forever? Optimising chemotherapeutic options for irradiation-free conditioning for paediatric acute lymphoblastic leukaemia. *Front Pediatr*. 2021;9:775485. https://doi.org/10.3389/fped.2021.775485.
3. Combarel D, Tran J, Delahousse J, Vassal G, Paci A. Individualizing busulfan dose in specific populations and evaluating the risk of pharmacokinetic drug-drug interactions. *Expert Opin Drug Metab Toxicol*. 2023;19(2):75–90. https://doi.org/10.1080/17425255.2023.2192924.
4. Seydoux C, Battegay R, Halter J, et al. Impact of busulfan pharmacokinetics on outcome in adult patients receiving an allogeneic hematopoietic cell transplantation. *Bone Marrow Transplant*. 2022;57(6):903–910. https://doi.org/10.1038/s41409-022-01641-6.
5. Ruutu T, van der Werf S, van Biezen A, et al. Use of busulfan in conditioning for allogeneic hematopoietic stem cell transplantation in adults: a survey by the Transplant Complications Working Party of the EBMT. *Bone Marrow Transplant*. 2019;54(12):2013–2019. https://doi.org/10.1038/s41409-019-0579-0.
6. Lawson R, Staatz CE, Fraser CJ, Hennig S. Review of the pharmacokinetics and pharmacodynamics of intravenous busulfan in paediatric patients. *Clin Pharmacokinet*. 2021;60(1):17–51. https://doi.org/10.1007/s40262-020-00947-2.
7. McCune JS, Navarro SL, Baker KS, et al. Prediction of busulfan clearance by predose plasma metabolomic profiling. *Clin Pharmacol Ther*. 2023;113(2):370–379. https://doi.org/10.1002/cpt.2794.
8. Seydoux C, Uppugunduri CRS, Medinger M, et al. Effect of pharmacokinetics and pharmacogenomics in adults with allogeneic hematopoietic cell transplantation conditioned with Busulfan. *Bone Marrow Transplant*. 2023;58:811–816. https://doi.org/10.1038/s41409-023-01963-z.
9. Yin J, Xiao Y, Zheng H, Zhang YC. Once-daily i.v. BU-based conditioning regimen before allogeneic hematopoietic SCT: a study of influence of GST gene polymorphisms on BU pharmacokinetics and clinical outcomes in Chinese patients. *Bone Marrow Transplant*. 2015;50(5):696–705. https://doi.org/10.1038/bmt.2015.14.
10. Michaud V, Tran M, Pronovost B, et al. Impact of GSTA1 polymorphisms on busulfan oral clearance in adult patients undergoing hematopoietic stem cell transplantation. *Pharmaceutics*. 2019;11(9):440. https://doi.org/10.3390/pharmaceutics11090440.
11. Kusama M, Kubota T, Matsukura Y, et al. Influence of glutathione S-transferase A1 polymorphism on the pharmacokinetics of busulfan. *Clin Chim Acta Int J Clin Chem*. 2006;368(1-2):93–98. https://doi.org/10.1016/j.cca.2005.12.011.
12. Kim MG, Kwak A, Choi B, Ji E, Oh JM, Kim K. Effect of glutathione S-transferase genetic polymorphisms on busulfan pharmacokinetics and veno-occlusive disease in hematopoietic stem cell transplantation: a meta-analysis. *Basic Clin Pharmacol Toxicol*. 2019;124(6):691–703. https://doi.org/10.1111/bcpt.13185.
13. Al-Riyami I, Al-Khabori M, Al Balushi K, et al. Impact of glutathione S-transferase polymorphisms on busulfan pharmacokinetics and outcomes of hematopoietic stem cell transplantation. *Ther Drug Monit*. 2022;44(4):527–534. https://doi.org/10.1097/FTD.0000000000000957.
14. Choi B, Kim MG, Han N, et al. Population pharmacokinetics and pharmacodynamics of busulfan with GSTA1 polymorphisms in patients undergoing allogeneic hematopoietic stem cell transplantation. *Pharmacogenomics*. 2015;16(14):1585–1594. https://doi.org/10.2217/pgs.15.98.
15. Ben Hassine K, Nava T, Théoret Y, et al. Precision dosing of intravenous busulfan in pediatric hematopoietic stem cell transplantation: results from a multicenter population pharmacokinetic study. *CPT Pharmacomet Syst Pharmacol*. 2021;10(9):1043–1056. https://doi.org/10.1002/psp4.12683.
16. Ansari M, Curtis PHD, Uppugunduri CRS, et al. GSTA1 diplotypes affect busulfan clearance and toxicity in children undergoing allogeneic hematopoietic stem cell transplantation: a multicenter study. *Oncotarget*. 2017;8(53):90852–90867. https://doi.org/10.18632/oncotarget.20310.
17. Nava T, Kassir N, Rezgui MA, et al. Incorporation of GSTA1 genetic variations into a population pharmacokinetic model for IV busulfan in paediatric hematopoietic stem cell transplantation. *Br J Clin Pharmacol*. 2018;84(7):1494–1504. https://doi.org/10.1111/bcp.13566.
18. Ansari M, Huezo-Diaz P, Rezgui MA, et al. Influence of glutathione S -transferase gene polymorphisms on busulfan pharmacokinetics and outcome of hematopoietic stem-cell transplantation in thalassemia pediatric patients. *Bone Marrow Transplant*. 2016;51(3):377–383. https://doi.org/10.1038/bmt.2015.321.
19. Seydoux C, Medinger M, Gerull S, et al. Busulfan-cyclophosphamide versus cyclophosphamide-busulfan as conditioning regimen before allogeneic hematopoietic cell transplantation: a prospective randomized trial. *Ann Hematol*. 2021;100(1):209–216. https://doi.org/10.1007/s00277-020-04312-y.
20. Mlakar V, Curtis PHD, Armengol M, et al. The analysis of GSTA1 promoter genetic and functional diversity of human populations. *Sci Rep*. 2021;11(1):5038. https://doi.org/10.1038/s41598-021-83996-2.
21. European Medicines Agency. Busilvex : summary of product characteristics. 2018. Available at: https://www.ema.europa.eu/en/medicines/human/EPAR/busilvex Accessed June 24, 2021.
22. Palmer J, McCune JS, Perales MA, et al. Personalizing busulfan-based conditioning: considerations from the American Society for Blood and Marrow Transplantation practice guidelines committee. *Biol Blood Marrow Transplant*. 2016;22(11):1915–1925. https://doi.org/10.1016/j.bbmt.2016.07.013.
23. Byon W, Smith MK, Chan P, et al. Establishing best practices and guidance in population modeling: an experience with an internal population pharmacokinetic analysis guidance. *CPT Pharmacomet Syst Pharmacol*. 2013;2:e51. https://doi.org/10.1038/psp.2013.26.
24. Nguyen L, Leger F, Lennon S, Puozzo C. Intravenous busulfan in adults prior to haematopoietic stem cell transplantation: a population pharmacokinetic study. *Cancer Chemother Pharmacol*. 2006;57(2):191–198. https://doi.org/10.1007/s00280-005-0029-0.
25. Mosteller RD. Simplified calculation of body-surface area. *N Engl J Med*. 1987;317(17):1098. https://doi.org/10.1056/NEJM198710223171717.
26. Dumont C, Lestini G, Le Nagard H, et al. PFIM 4.0, an extended R program for design evaluation and optimization in nonlinear mixed-effect models. *Comput*

Methods Programs Biomed. 2018;156:217–229. https://doi.org/10.1016/j.cmpb.2018.01.008.
27. Dubovitskaya A, Buclin T, Schumacher M, Aberer K, Thoma Y. TUCUXI: an intelligent system for personalized medicine from individualization of treatments to research databases and back. In: Proceedings of the 8th ACM International Conference on Bioinformatics, *Computational Biology,and Health Informatics - ACM-BCB '17*. Association for Computing Machinery; 2017:223–232. https://doi.org/10.1145/3107411.3107439.
28. Jamei M, Marciniak S, Feng K, Barnett A, Tucker G, Rostami-Hodjegan A. The Simcyp population-based ADME simulator. *Expert Opin Drug Metab Toxicol*. 2009;5(2):211–223. https://doi.org/10.1517/17425250802691074.
29. PubChem. Busulfan. 2023. Available at: https://pubchem.ncbi.nlm.nih.gov/compound/2478. Accessed June 16, 2023.
30. DrugBank. Busulfan. 2023. Available at: https://go.drugbank.com/drugs/DB01008 Accessed June 16, 2023.
31. Dilo A, Daali Y, Desmeules J, Chalandon Y, Uppugunduri CRS, Ansari M. Comparing dried blood spots and plasma concentrations for busulfan therapeutic drug monitoring in children. *Ther Drug Monit*. 2020;42(1):111–117. https://doi.org/10.1097/FTD.0000000000000673.
32. Berezhkovskiy LM. Volume of distribution at steady state for a linear pharmacokinetic system with peripheral elimination. *J Pharm Sci*. 2004;93(6):1628–1640. https://doi.org/10.1002/jps.20073.
33. Bredschneider M, Klein K, Mürdter TE, et al. Genetic polymorphisms of glutathione S-transferase A1, the major glutathione S-transferase in human liver: consequences for enzyme expression and busulfan conjugation. *Clin Pharmacol Ther*. 2002;71(6):479–487. https://doi.org/10.1067/mcp.2002.124518.
34. Diestelhorst C, Boos J, McCune JS, Russell J, Kangarloo SB, Hempel G. Physiologically based pharmacokinetic modelling of Busulfan: a new approach to describe and predict the pharmacokinetics in adults. *Cancer Chemother Pharmacol*. 2013;72(5):991–1000. https://doi.org/10.1007/s00280-013-2275-x.
35. Raftos JE, Whillier S, Kuchel PW. Glutathione synthesis and turnover in the human erythrocyte. *J Biol Chem*. 2010;285(31):23557–23567. https://doi.org/10.1074/jbc.M109.067017.
36. Savic RM, Karlsson MO. Importance of shrinkage in empirical bayes estimates for diagnostics: problems and solutions. *AAPS J*. 2009;11(3):558–569. https://doi.org/10.1208/s12248-009-9133-0.
37. American Food and Drug Administration. Busulfex Prescribing information. 2023. Available at: https://www.accessdata.fda.gov/drugsatfda_docs/label/2015/020954s014lbl.pdf. Accessed June 23, 2023.
38. Bubalo J, Carpenter PA, Majhail N, et al. Conditioning chemotherapy dose adjustment in obese patients: a review and position statement by the American Society for Blood and Marrow Transplantation practice guideline committee. *Biol Blood Marrow Transplant*. 2014;20(5):600–616. https://doi.org/10.1016/j.bbmt.2014.01.019.
39. Griffin SP, Wheeler SE, Wiggins LE, Murthy HS, Hsu JW, Richards AI. Pharmacokinetic and clinical outcomes when ideal body weight is used to dose busulfan in obese hematopoietic stem cell transplant recipients. *Bone Marrow Transplant*. 2019;54(2):218–225. https://doi.org/10.1038/s41409-018-0240-3.
40. Slattery JT, Sanders JE, Buckner CD, et al. Graft-rejection and toxicity following bone marrow transplantation in relation to busulfan pharmacokinetics. *Bone Marrow Transplant*. 1995;16(1):31–42.
41. Dix SP, Wingard JR, Mullins RE, et al. Association of busulfan area under the curve with veno-occlusive disease following BMT. *Bone Marrow Transplant*. 1996;17(2):225–230.
42. Andersson BS, Thall PF, Madden T, et al. Busulfan systemic exposure relative to regimen-related toxicity and acute graft-versus-host disease: defining a therapeutic window for i.v. BuCy2 in chronic myelogenous leukemia. *Biol Blood Marrow Transplant*. 2002;8(9):477–485. https://doi.org/10.1053/bbmt.2002.v8.pm12374452.
43. Bartelink IH, Lalmohamed A, van Reij EML, et al. Association of busulfan exposure with survival and toxicity after haemopoietic cell transplantation in children and young adults: a multicentre, retrospective cohort analysis. *Lancet Haematol*. 2016;3(11):e526–e536. https://doi.org/10.1016/S2352-3026(16)30114-4.
44. McCune JS, Gibbs JP, Slattery JT. Plasma concentration monitoring of busulfan: does it improve clinical outcome? *Clin Pharmacokinet*. 2000;39(2):155–165. https://doi.org/10.2165/00003088-200039020-00005.
45. Andersson BS. Fludarabine-IV busulfan, dose-intensity and progression-free survival: are we finally finding the way to reach a consensus opinion?: Higher busulfan dose intensity appears to improve leukemia-free and overall survival in AML allografted in CR2: an analysis from the acute leukemia working party of the European group for blood and marrow transplantation. *Leuk Res*. 2016;41:5–6. https://doi.org/10.1016/j.leukres.2015.11.015.
46. Chen T, Chen C, He X, Guo J, Liu M, Zheng B. Fixed-dose administration and pharmacokinetically guided adjustment of busulfan dose for patients undergoing hematopoietic stem cell transplantation: a meta-analysis and cost-effectiveness analysis. *Ann Hematol*. 2022;101(3):667–679. https://doi.org/10.1007/s00277-021-04733-3.
47. Davis JM, Ivanova A, Chung Y, et al. Evaluation of a test dose strategy for pharmacokinetically-guided busulfan dosing for hematopoietic stem cell transplantation. *Biol Blood Marrow Transplant*. 2019;25(2):391–397. https://doi.org/10.1016/j.bbmt.2018.09.017.
48. Salman B, Al-Za'abi M, Al-Huneini M, et al. Therapeutic drug monitoring-guided dosing of busulfan differs from weight-based dosing in hematopoietic stem cell transplant patients. *Hematol Oncol Stem Cell Ther*. 2017;10(2):70–78. https://doi.org/10.1016/j.hemonc.2017.03.003.
49. Dunlap TC, Weiner DL, Kemper RM, et al. Utilization of a population pharmacokinetic model to improve a busulfan test-dose strategy in allogeneic hematopoietic cell transplant recipients. *J Clin Pharmacol*. 2023;63(9):1026–1035. https://doi.org/10.1002/jcph.2257.
50. Simon N, Coiteux V, Bruno B, et al. Adaptation des doses de médicament des conditionnements de greffe de cellules souches hématopoïétiques dans des populations avec comorbidité : obésité, maladie rénale chronique ou hépatopathie : recommandations de la Société francophone de greffe de moelle et de thérapie cellulaire (SFGM-TC). *Bull Cancer (Paris)*. 2017;104(suppl 12):S99–S105. https://doi.org/10.1016/j.bulcan.2017.07.010.
51. Langenhorst JB, Boss J, van Kesteren C, et al. A semi-mechanistic model based on glutathione depletion to describe intra-individual reduction in busulfan clearance. *Br J Clin Pharmacol*. 2020;86(8):1499–1509. https://doi.org/10.1111/bcp.14256.
52. Alkazemi D, Rahman A, Habra B. Alterations in glutathione redox homeostasis among adolescents with obesity and anemia. *Sci Rep*. 2021;11(1):3034. https://doi.org/10.1038/s41598-021-82579-5.